

Analysis of precompound processes in (p,n) reactions with the statistical multistep direct emission theory

R. Bonetti, M. Camnasio, and L. Colli Milazzo

Physics Institute of the University of Milan, Italy

P. E. Hodgson

Nuclear Physics Laboratory, Oxford, United Kingdom

(Received 3 November 1980)

The fully quantum-mechanical statistical multistep direct emission theory of Feshbach, Kerman, and Koonin is used to analyze the differential cross sections of (p,n) reactions on ^{48}Ca , ^{90}Zr , ^{120}Sn , and ^{208}Pb from 25 to 45 MeV. The interacting particles are described by distorted waves and the interactions inside the nucleus are described by a single-particle model. The absolute magnitudes, as well as the angular variations of the continuum spectra, are well reproduced and the relative contributions of single and multistep processes are evaluated.

[NUCLEAR REACTIONS ^{48}Ca , ^{90}Zr , ^{120}Sn , ^{208}Pb (p,n) . Calculated cross sections and angular distributions. Deduced two-body interaction strength.]

I. INTRODUCTION

In recent years there have been many attempts to understand the continuum spectra of the energetic particles that are emitted predominantly in the forward direction from many reactions at intermediate energies. This work uses the concepts of precompound emission and attributes these particles to processes occurring after the initial interaction but before the attainment of statistical equilibrium. The earlier theories used classical and semiclassical concepts and were all able with some adjustment of parameters to fit the energy variation of the angle-integrated cross section.¹ Subsequently, some calculations have been made of the angular distributions of the particles emitted in these reactions. Mantzouranis *et al.*,² using a quantum-statistical master equation approach, were able to calculate the angular distribution for a number of reactions but still using the concepts of the exciton model with phenomenologically adjusted parameters. Tamura *et al.*³ extended into the continuum the multistep direct theory originally used to describe transitions to individual final states. In this work they retain an essentially microscopic description of the transition matrix elements, being able to calculate the first and second step cross section of a number of reactions.

A complete quantum-mechanical theory has recently been formulated by Feshbach, Kerman, and Koonin.⁴ This theory distinguishes two types of precompound processes, one that involves bound excited states of the intermediate nucleus, called statistical multistep compound emission (SMCE), and another that involves unbound excited states of the intermediate nucleus, called sta-

tistical multistep direct emission (SMDE). These two mechanisms are characterized by the angular distribution of the emitted particles; the former (SMCE) giving angular distributions symmetric about 90° and the latter (SMDE) giving angular distributions peaked in the forward direction.

Many measurements have been made of reactions showing the general characteristics of SMDE, in particular (p,n) , (p,p') , and (p,α) at energies above 30 MeV over the whole range of nuclei. A particular useful set for detailed analysis with the SMDE theory is the (p,n) data at 45 MeV obtained by Galonsky *et al.*⁵ They measured the energy spectrum and the angular distributions of the emitted neutrons for many nuclei from calcium to lead. The results of a preliminary analysis of $^{120}\text{Sn}(p,n)$ at 45 MeV have already been published.⁶ In this paper we extend the analysis to other target nuclei and examine in detail the optimum choice of parameters.

II. THEORETICAL FORMULATION

The quantum mechanical theory of the statistical multistep direct process retains many of the concepts already used in the semiclassical theories of pre-equilibrium emission. The incident kinetic energy is spread through the target nucleus by the two-body residual interaction, and the excited nuclear states are characterized by their number of "excitons," or particle-hole excitations. The class of states labeled P_n contains $2n+1$ excitons, one of which is in the continuum. The first hypothesis in this theory is the chaining hypothesis, which restricts interactions to classes of states with n differing by unity. The second assumption is that the only matrix elements that interfere

constructively after averaging are those with the same change of momentum as the particle in the continuum. This assumption is a particular formulation of the random phase hypothesis, which is usually made in the statistical theory of nuclear reactions.

Another fundamental concept in the theory is the "exit mode." Since this is a theory of the continuum part of the spectrum, we are concerned only with energy averages over the residual nuclear states, not with the states individually. In the theory the final wave function is decomposed into configurations belonging to the various components P_n of the partitioned P space (this being the space of "open" states, i.e., those with at least one particle in the continuum). These configurations are referred to as exit modes. Each nuclear state belonging to the chain of states formed by the residual two-body interaction

can make transition to an exit mode m through the same two-body interaction, where m can be $n \pm 1$ according to the chaining hypothesis.

The double differential cross section for a reaction from a state having a particle of momentum \vec{k}_i to one of momentum \vec{k}_f is the sum of the single-step and multistep processes

$$\left[\frac{d^2\sigma(\vec{k}_i, \vec{k}_f)}{dU d\Omega} \right]_{\text{direct}} = \left[\frac{d^2\sigma(\vec{k}_i, \vec{k}_f)}{dU d\Omega} \right]_{\text{single step}} + \left[\frac{d^2\sigma(\vec{k}_i, \vec{k}_f)}{dU d\Omega} \right]_{\text{multistep}}. \quad (2.1)$$

With the assumptions already mentioned, the multistep process has the cross section

$$\left[\frac{d^2\sigma(\vec{k}_i, \vec{k}_f)}{dU d\Omega} \right]_{\text{multistep}} = \sum_n \sum_{m=n-1}^{n+1} \int \frac{d\vec{k}_1}{(2\pi)^3} \int \frac{d\vec{k}_2}{(2\pi)^3} \dots \int \frac{d\vec{k}_n}{(2\pi)^3} \frac{d^2W_{m,n}(\vec{k}_f, \vec{k}_n)}{dU_f d\Omega_f} \frac{d^2W_{n,n-1}(\vec{k}_n, \vec{k}_{n-1})}{dU_n d\Omega_n} \dots \frac{d^2W_{2,1}(\vec{k}_2, \vec{k}_1)}{dU_2 d\Omega_2} \times \left(\frac{d^2\sigma(\vec{k}_1, \vec{k}_1)}{dU_1 d\Omega_1} \right)_{\text{single step}}, \quad (2.2)$$

where m labels the exit mode and n the stage. In the region of continuum states the Fermi Golden Rule for the transition probability from the $(n-1)$ th to the n th stage, when the particle changes its momentum from \vec{k}_{n-1} to \vec{k}_n , is given by

$$\frac{d^2W_{n,n-1}(\vec{k}_n, \vec{k}_{n-1})}{dU_n d\Omega_n} = 2\pi^2 \rho(\vec{k}_n) \rho_n(U) \times \langle |v_{n,n-1}(\vec{k}_n, \vec{k}_{n-1})|^2 \rangle, \quad (2.3)$$

where $\rho(\vec{k}_n) = mk/(2\pi)^3 \hbar^2$ is the density of states of the particle in the continuum, $\rho_n(U)$ is the level density of the residual nucleus at excitation energy U , and $v_{n,n-1}(\vec{k}_n, \vec{k}_{n-1})$ is the matrix element describing the transition from a state $n-1$ to a state n when the particle in the continuum changes its momentum from \vec{k}_{n-1} to \vec{k}_n . This matrix element may be evaluated using the distorted-wave Born approximation (DWBA) expression

$$v_{a,b}(\vec{k}_i, \vec{k}_f) = \int \chi_a^{(-)*} \langle \psi_f | V(r) | \psi_i \rangle \chi_b^{(+)} d\vec{r}, \quad (2.4)$$

where $V(r)$ is the effective interaction for the

transition, $\chi_a^{(-)}$ and $\chi_b^{(+)}$ are the incoming and outgoing distorted waves, and ψ_i and ψ_f are the initial and final nuclear states. To ensure that all the transition strength is included, we take the spectroscopic factors to be unity throughout. Since we need the matrix element describing the average transition probability to many final states in the energy interval dU , an appropriate averaging procedure has to be given. Since the interference terms are expected on the average to cancel, we assume that the orbital angular momenta L contribute incoherently, so that the average value of the squared matrix element can be written

$$\langle |v(\vec{k}_i, \vec{k}_f)|^2 \rangle = \sum_L (2L+1) \langle |v(\vec{k}_i, \vec{k}_f)_L|^2 \rangle R_2(L), \quad (2.5)$$

where $R_2(L)$ is the spin distribution function of the residual nucleus levels, acting as a weighting factor. It must be pointed out that $\sum_L R(L)(2L+1) = 1$. In the same way, the averaged single-step cross section, which acts as the source term in the expression (2.2) for the multistep cross section, is given by

TABLE I. Optical model parameters used in the DWBA calculations. The potential depths are in MeV, the diffuseness and radius parameters in fm. The potential form factors are the same as in Becchetti-Greenlees (Ref. 7). The depths of the real Woods-Saxon potential used for the bound-state calculations are adjusted to the nucleon binding energy \pm the excitation energy of the levels being considered.

Target	V_r	a_R	r_{0r}	W_v	a_i	r_{0i}	W_{sf}	V_{so}	a_{so}	r_{so}	Bound States	
											a_r	r_{0r}
^{48}Ca	p 60.2 - 0.32E	0.75	1.17	0.22E - 2.7	0.626	1.32	13.8 - 0.25E	6.2	0.75	1.01	0.5	1.1
	n 52.3 - 0.32E			0.22E - 1.56	0.58	1.26	11 - 0.25E					
^{90}Zr	p 60.2 - 0.32E	0.75	1.17	0.22E - 2.7	0.587	1.32	13.1 - 0.25E	6.2	0.75	1.01	0.5	1.1
	n 53.6 - 0.32E			0.22E - 1.56	0.58	1.26	11.6 - 0.25E					
^{120}Sn	p 62 - 0.32E	0.75	1.17	0.22E - 2.7	0.626	1.32	13.8 - 0.25E	6.2	0.75	1.01	0.6	1.2
	n 52.3 - 0.32E			0.22E - 1.56	0.58	1.26	11 - 0.25E					
^{208}Pb	p 64.6 - 0.32E	0.75	1.17	0.22E - 2.7	0.658	1.32	14.3 - 0.25E	6.2	0.75	1.01	0.6	1.2
	n 51.2 - 0.32E			0.22E - 1.56	0.58	1.26	10.4 - 0.25E					

$$\left[\frac{d^2\sigma(\mathbf{k}_i, \mathbf{k}_f)}{dU d\Omega} \right]_{\text{single step}} = \sum_L (2L+1) \rho_2(U) R_2(L) \times \left\langle \left(\frac{d\sigma}{d\Omega} \right)_L \right\rangle, \quad (2.6)$$

where the suffix of $\rho_2(U)$ corresponds to the number of the excitons in the residual nucleus after the first interaction.

III. APPLICATION TO (p, n) REACTIONS

To apply the formalism described in Sec. II for calculating the cross section of (p, n) reactions on several nuclei we neglect the intrinsic spin of the incident and final particles, so that since all the targets are even-even, the only contribution to the spins of the final states comes from the transferred angular momentum. For each transferred L value it is possible to calculate microscopically the inelastic cross section as a function of angle, and for given values of the incoming and outgoing energies, for all possible pairs of initial and final bound states compatible with energy conservation. A single-particle shell model is used to describe the states. The average of all these cross sections gives as a result $\langle d\sigma/d\omega \rangle_L$ for each L value, independent of the details of nuclear structure.

In the present calculations we use a Yukawa potential of range 1.0 fm for $V(r)$ and calculate the incident and outgoing distorted waves using the potentials of Becchetti and Greenlees.⁷ The energy dependence of these potentials was found consistent with the potentials tabulated by Perey and Perey,⁸ at least in the energy range of the present calculations.

The bound state wave functions were generated

in a real Woods-Saxon potential whose surface diffuseness and radius parameters are shown in Table I. Table I also shows the optical model parameters which have been used. The strength of the Yukawa potential is the only free parameter.

The results of a typical set of calculations for a particular L value are shown in Fig. 1. These

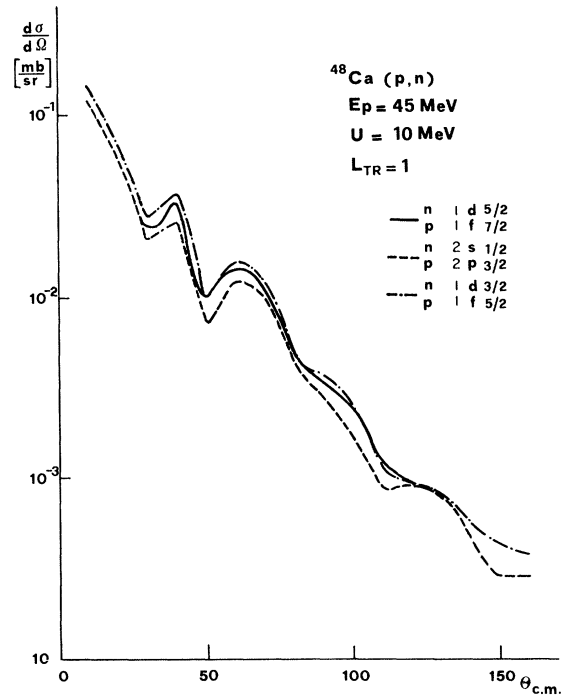


FIG. 1. Calculated differential cross sections for some typical transitions in ^{48}Ca at 45 MeV between shell-model states corresponding to $\Delta L = 1$, showing their overall similarity.

cross sections are then averaged to obtain $\langle d\sigma/d\omega \rangle_L$.

To calculate the single-step contribution (2.6) we use for the \bar{n} -exciton state level density the Ericson expression⁹

$$\rho_{\bar{n}}(U) = g(gU)^{\bar{n}-1}/p! h! (\bar{n}-1)! \quad (\bar{n}=p+h) \quad (3.1)$$

and for the spin distribution function^{4,9}

$$R_{\bar{n}}(L) = \frac{2L+1}{\sqrt{\pi} \bar{n}^{3/2} \sigma^3} \exp\left[-\frac{(L+\frac{1}{2})^2}{\bar{n}\sigma^2}\right], \quad (3.2)$$

where σ is the spin cutoff parameter, as usually defined.⁹ These expressions are also used for the calculation of the transition probabilities (2.3) and hence of the multistep contribution (2.2). These calculations may be extended directly to calculate the cross section of the multistep process because the differential transition probabilities (2.3) do not depend on the stage of the chain. In this calculation, the level density $\rho_n(U)$ describes the final states of the interaction when a particle in the continuum with momentum \vec{k}_{n-1} collides with a bound nucleon, changing its momentum to \vec{k}_n and creating a particle-hole pair. The final state density is therefore that of a particle-hole pair, that is, $\rho_2(U)$ for all stages of the chain.

In the multistep calculation the averaged expression (2.5) is inserted in (2.3) and then integrated over all intermediate energies and angles. The calculation of subsequent steps is straightforward since the source term of each step comes from the calculation of the previous steps.

Despite this, the calculation is time consuming because it requires V_{ab} at each value of the incoming and outgoing energies compatible with energy conservation and for each angle and transferred L value. To limit the number of calculations we have varied the energy in steps of 4 or 6 MeV, and the angle in steps of 10° . In principle, the calculation should be made considering both protons and neutrons at intermediate stages but in practice, due to the similarity of their optical potentials, it was found that there is no appreciable difference in the angular distributions if this distinction is ignored, retaining the correct wave functions only for the initial and final particles. To obtain the absolute magnitudes, we have used the result of Austin¹⁰ that the interaction is about four times as strong between unlike particles as between like particles. Thus in the multistep calculation we have used an appropriately averaged value of the interaction strength.

In this way we have calculated the continuum spectra and related angular distributions of the (p, n) reactions on ^{48}Ca , ^{90}Zr , and ^{208}Pb at 45 MeV. In the case of ^{120}Sn , calculations at 45 MeV

have been previously reported⁶; they have been extended here for incident energies of 25 and 35 MeV.

IV. DISCUSSION OF RESULTS AND CONCLUSIONS

The results of these calculations are compared with the experimental data in Figs. 2–6. Table II shows the relevant quantities which have been used, together with some of the results obtained.

It must be emphasized that in all these calculations there is only one adjustable parameter, the strength V_0 of the Yukawa potential, which represents the residual interaction developing the Feshbach chain. Even in this case, as will be discussed below, the value chosen is not only consistent with other work, but is largely determined by the requirement of simultaneous fit to the absolute magnitudes and to the angular distributions.

The other quantities are either calculated *a priori*, such as the spin cutoff parameter σ , or taken from the literature, such as the single particle level density parameters a , used in the calculation of $g = 6a/\pi^2$. The former was calculated using the prescriptions of Feshbach *et al.*,⁴ at an average value of the excitation energy $U = 16$ MeV. The latter were taken from the slow-neutron resonances analysis of Facchini *et al.*,¹¹ with the exception of the one for the double-magic nucleus ^{208}Pb . For this nucleus indeed, the value measured at ~ 8 MeV excitation energy is $\sim 9 \text{ MeV}^{-1}$, much smaller than the one we have used. It is well known, however, that the shell effect causing the decrease in the effective level density parameter is washed out at increasing excitation energy. Williams *et al.*¹² have found that at ~ 40 MeV excitation energy the a value for ^{208}Pb reaches $\sim 25 \text{ MeV}^{-1}$, a value that is typical for this mass region.

The V_0 values obtained from the best fit are remarkably constant over the large mass range under consideration (Table II). They are perfectly compatible with the value of the central part of the effective interaction $V_0 = 27.9 \pm 3.5$ which was determined by Austin¹⁰ from a wide analysis of inelastic scattering reactions leading to discrete levels of the final nucleus.

It should be pointed out that since V_0 operates at each step, the final m -step cross section is proportional to V_0^{2m} . The value of V_0 thus strongly determines the relative importance of the contributions from the different steps, as well as the absolute value of the cross section. It is thus not just a normalization coefficient, because it also strongly affects the spectral shapes and angular distributions. The overall agreement with the experimental data shown in Figs. 2–6

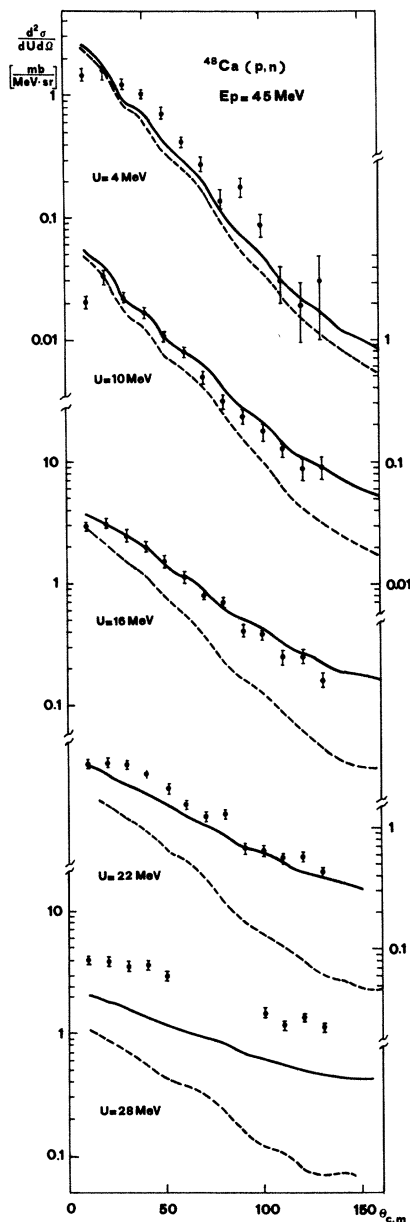


FIG. 2. Comparison between calculated and experimental differential cross sections for the $^{48}\text{Ca}(p, n)$ reaction at several excitation energies of the residual nucleus. At the highest excitation energy ($u=28$ MeV), the experimental cross section exceeds the calculated value due to the presence of multiple particle emission. --- single-step contribution; — total.

with an essentially constant value of V_0 thus confirms the overall validity of the theory.

These calculations show the importance of the multistep processes in the Feshbach chain. More precisely, Table II shows that at 45 MeV incident

energy about one half of the integrated cross section, for all nuclei under consideration, is due to multistep processes. This quantity decreases, as expected, with decreasing incident energy. Figure 3 also shows that this multistep contribution depends strongly on the emission angle; as this angle and the residual excitation energy increases, so does the contribution of multistep processes.

The results also show that rather few steps contribute to the reactions—it was never necessary to include more than six. Calculations with as many steps as required can be performed without difficulty, so the analysis is easy to extend to higher incident energies.

Despite the general success, some disagreements do exist. There is often some strength missing at high excitation energy, as shown by Figs. 2–6. This may be due to some contributions from multiple emission, which is included in the measurements but not calculated here. At low incident energy, as shown by Fig. 6 for ^{120}Sn at 25 MeV, the spectrum is not well fitted by the SMDE calculation, probably because SMCE, which is likely to be present at this incident energy, was not included in our calculations. This interpretation receives support from the general isotropy of the angular distribution of the difference $\sigma_{\text{exp}} - \sigma_{\text{calc}}$, as shown in Fig. 7.

It is interesting at this time to compare this calculation with other theories concerned with the extension of the direct effect calculations to the continuum part of the spectrum. A quite successful one seems to be that of Tamura *et al.*³ They calculate the average cross section by summing up the DWBA cross sections obtained for all possible particle-hole configurations at a given excitation in the frame of the single particle shell model.

In this way, they obtain the continuum energy spectra and angular distributions of the particles emitted by one- and two-step processes in a number of reactions. In particular, they are able to reproduce the (p, p') scattering at 62 MeV with only two steps, and practically all the cross section at $U=10$ – 20 MeV with the single step contribution. These results are not consistent with the results of the SMDE theory, which have been discussed above. On the other hand, Tsai and Bertsch¹³ calculate the same (p, p') reactions as Tamura *et al.* in the frame of the random-phase approximation (RPA) theory of the target excitation and using a sum rule to test the values of the multipole transition strengths they obtain from the DWBA calculations. In this way they find that only about 25% of the experimental strength can be accounted for by one-step contributions.

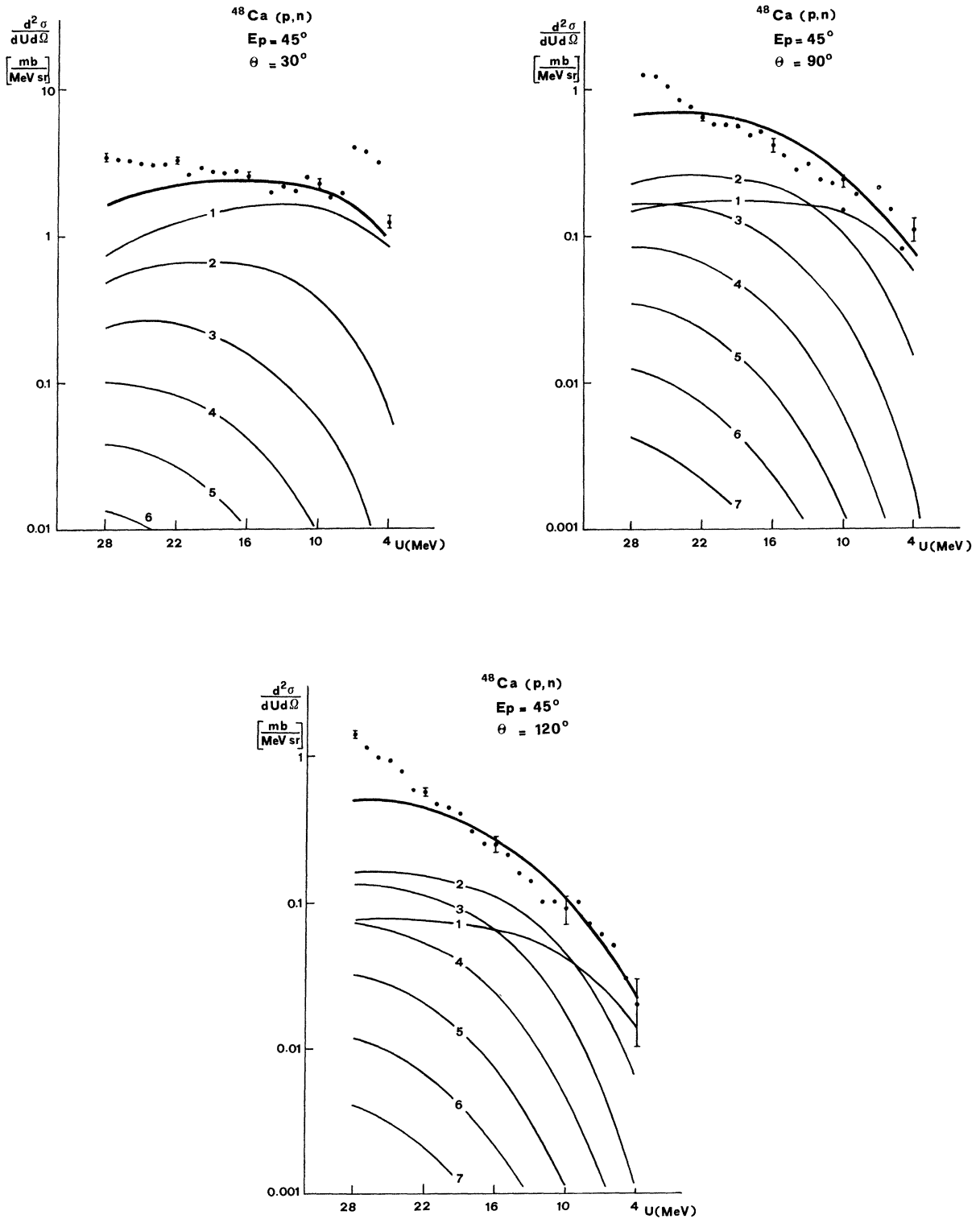


FIG. 3. Comparison between calculated and experimental energy spectra for $^{48}\text{Ca}(p,n)$ at several energies showing the contributions of various steps. The short fall at the higher excitation energies is attributed to multiparticle emission. It is notable that in the backward direction the two-step and even the three-step cross section is sometimes greater than the one step cross section.

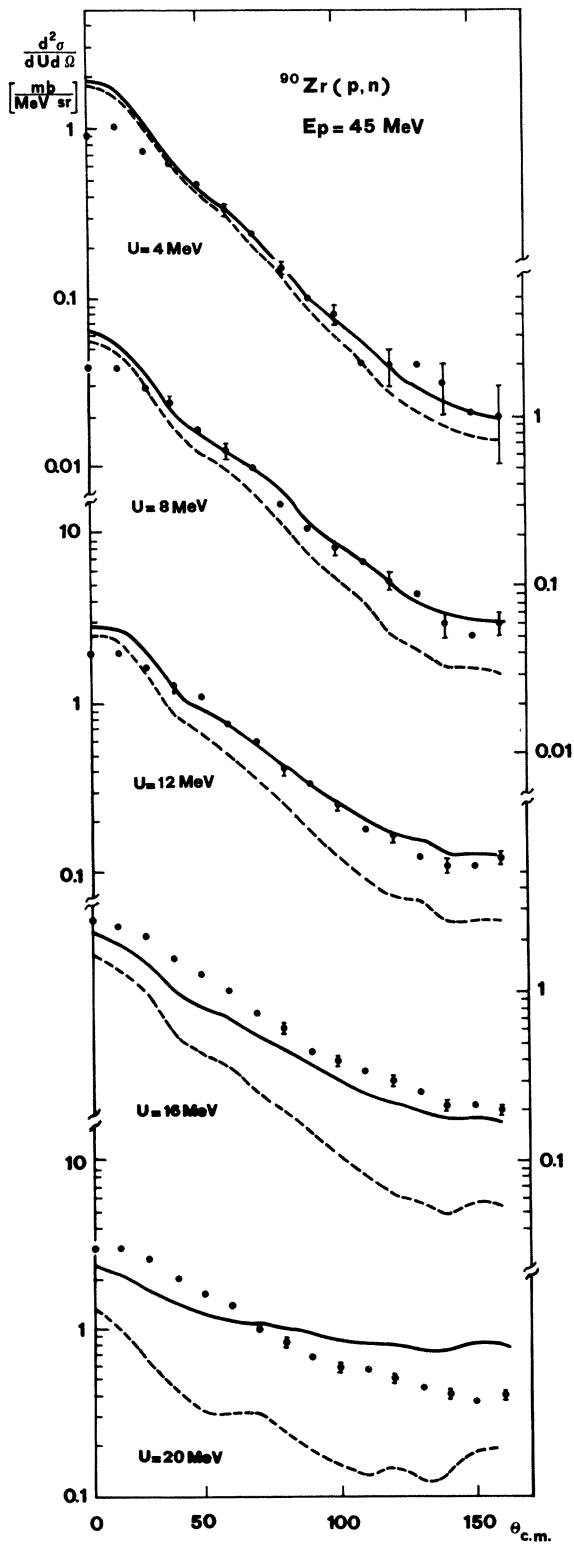


FIG. 4. Comparison between calculated and experimental differential cross sections for the $^{90}\text{Zr}(p, n)$ reaction. --- single-step contribution; — total.

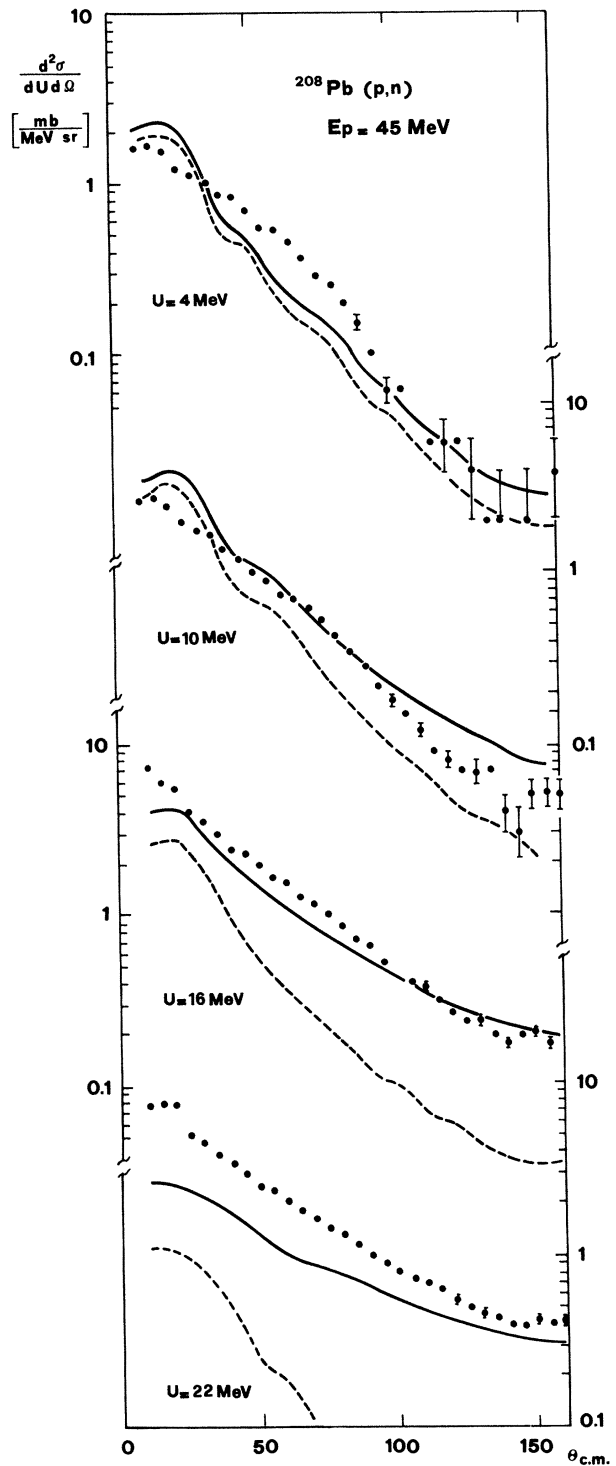


FIG. 5. Comparison between calculated and experimental differential cross sections for the $^{208}\text{Pb}(p, n)$ reaction. --- single-step contribution; — total.

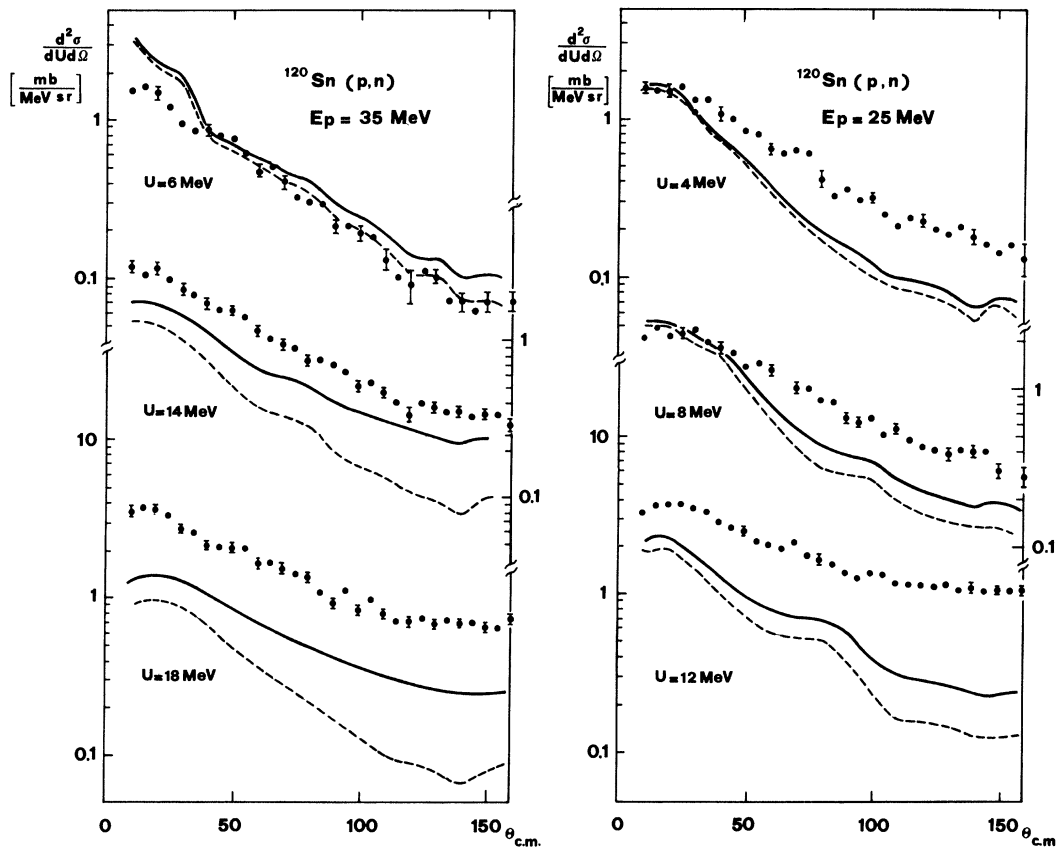


FIG. 6. Comparison between calculated and experimental differential cross sections for the $^{120}\text{Sn}(p,n)$ reaction at 35 and 25 MeV incident proton energy. --- single-step contribution; — total. The short fall at the lower energy is attributed to the omission in the calculation of the statistical multistep compound process.

TABLE II. The columns show in order: the spin cutoff parameter; the single-particle level density parameter; the strength of the 1-fm-range Yukawa potential describing the interaction between unlike nucleons, used for the single-step calculations; the same, but averaged over all possible nucleon-nucleon interactions used for the multistep calculations; and the ratio of the single step cross section with the total cross section.

Target	σ	a (MeV^{-1})	V_0 (MeV)	\bar{V}_0 (MeV)	σ_1/σ_{tot}
^{48}Ca $E_p = 45$ MeV	1.4	7.4	27.5	15.5	0.55
^{90}Zr $E_p = 45$ MeV	1.9	10	27.5	17	0.55
^{120}Sn $E_p = 25$ MeV	2.5	16	27.5	16	0.82
^{120}Sn $E_p = 35$ MeV	2.5	16	27.5	16	0.72
^{208}Pb $E_p = 45$ MeV	3.4	13	27	15	0.47

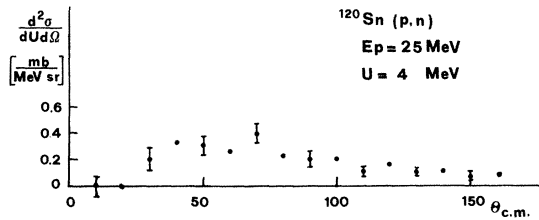


FIG. 7. Difference between the experimental and theoretical cross section for the $^{120}\text{Sn}(p, n)$ reaction at 25 MeV. The isotropic behavior of this difference supports its interpretation as due to the statistical multistep compound process.

This result is consistent with our calculations which have been done at lower incident energy.

In conclusion, we believe we have shown the validity of the SMDE theory. Its applicability to calculate particular reactions depends, of course,

on how easy and reliable the corresponding DWBA calculations are. We believe that this theory can be used as a sensitive tool for studying the two-body residual interaction between nucleons, due to the critical way it determines the cross section of reactions to the continuum at intermediate energies.

ACKNOWLEDGMENTS

We want to thank Prof. H. Feshbach and Prof. T. Tamura for helpful discussions, and Prof. A. Galonsky for kindly providing us with the unpublished data of (p, n) reactions. This work was supported by the British Council-Consiglio Nazionale delle Ricerche Academic link, by the Istituto Nazionale di Fisica Nucleare, Milan, and by the North Atlantic Treaty Organization (Research Grant No. 184.80).

¹M. Blann, *Annu. Rev. Nucl. Sci.* **25**, 123 (1975).

²G. Mantzouranis, D. Agassi, and H. A. Weidenmuller, *Phys. Lett.* **57B**, 220 (1975); G. Mantzouranis, *Phys. Rev. C* **14**, 2018 (1976).

³T. Tamura, T. Udagawa, D. H. Feng, and K.-K. Kan, *Phys. Lett.* **66B**, 109 (1977).

⁴H. Feshbach, A. Kerman, and S. Koonin, *Ann. Phys. (N.Y.)* **125**, 429 (1980).

⁵M. Blann, R. R. Doering, A. Galonsky, D. M. Patterson, and F. E. Serr, *Nucl. Phys.* **A257**, 15 (1976); R. R. Doering, A. Galonsky, D. M. Patterson, and F. E. Serr, Michigan State University Report MSUCP-29 (1976).

⁶L. Avaldi, R. Bonetti, and L. Colli Milazzo, *Phys. Lett.* **94B**, 463 (1980).

⁷F. D. Becchetti and G. W. Greenlees, *Phys. Rev.* **182**, 1190 (1969).

⁸C. M. Perey and F. G. Perey, *Nucl. Data Tables* **17**, 1 (1976).

⁹T. Ericson, *Advan. Phys.* **9**, 425 (1960).

¹⁰S. M. Austin, in *The (p, n) Reaction and the Nucleon-Nucleon Force*, Proceedings of a conference, Telluride, Colorado, 1979, edited by C. D. Goodman, S. M. Austin, and S. D. Bloom (Plenum, New York, 1980).

¹¹U. Facchini and E. Saetta Menichella, *Energ. Nucl. (Milan)* **15**, 54 (1968).

¹²F. C. Williams, J. C. Chan, and J. R. Huizenga, *Nucl. Phys.* **A187**, 225 (1972).

¹³S. Tsai and G. F. Bertsch, *Phys. Rev. C* **11**, 1634 (1975); G. F. Bertsch, in *Proceedings of the International Workshop on Reaction Models for Continuous Spectra of Light Particles, Bad Honnef, 1978* (Institut für Strahlen und Kernphysik, Bonn, 1979).